Available online at www.sciencedirect.com
SCIENCE DIRECT®
Journal of Sound and Vibration 282 (2005) 215–230
JOURNAL OF SOUND AND VIBRATION
www.elsevier.com/locate/jsvi

A new method to extract modal parameters using output-only responses

Byeong Hwa Kim[a], Norris Stubbs[b], Taehyo Park[a,*]

[a]*Computational Solid & Structural Mechanics Laboratory, Department of Civil Engineering, Hanyang University, 17 Haengdang-dong, Seoul 133-791, Korea*
[b]*Department of Civil Engineering, MS 3136, Texas A&M University, College Station, TX 77843, USA*

Received 31 July 2003; received in revised form 27 October 2003; accepted 18 February 2004
Available online 22 September 2004

Abstract

This work proposes a new output-only modal analysis method to extract mode shapes and natural frequencies of a structure. The proposed method is based on an approach with a single-degree-of-freedom in the time domain. For a set of given mode-isolated signals, the un-damped mode shapes are extracted utilizing the singular value decomposition of the output energy correlation matrix with respect to sensor locations. The natural frequencies are extracted from a noise-free signal that is projected on the estimated modal basis. The proposed method is particularly efficient when a high resolution of mode shape is essential. The accuracy of the method is numerically verified using a set of time histories that are simulated using a finite-element method. The feasibility and practicality of the method are verified using experimental data collected at the newly constructed King Storm Water Bridge in California, United States.

1. Introduction

Critical structures such as bridges, aircrafts, spacecrafts and offshore platforms are designed for specified service lives. Unanticipated hostile loading environments may decrease the service life of

*Corresponding author. Tel.: +82-2-2290-0321; fax: +82-2-2293-9977.
E-mail address: cepark@hanyang.ac.kr (T. Park).

0022-460X/$ - see front matter © 2004 Elsevier Ltd. All rights reserved.
doi:10.1016/j.jsv.2004.02.026

Nomenclature

$c_i(t)$	the ith modal contribution factor of displacement at time t
$\dot{c}_i(k)$	the ith modal contribution factor of velocity at the sample time k
$\ddot{c}_i(t)$	the ith modal contribution factor of acceleration at time t
$\ddot{c}_i(k)$	the ith modal contribution factor of acceleration at the sample time k
$\ddot{\mathbf{c}}_i$	the $N \times 1$ matrix containing $\ddot{c}_i(k)$ with $k = 1, \ldots, N$
$d_j(k)$	the jth noise contribution factor at the sample time k
$\ddot{\mathbf{d}}_j$	the $N \times 1$ matrix containing $\ddot{d}_j(k)$ with $k = 1, \ldots, N$
$\ddot{\boldsymbol{\varepsilon}}_t(k)$	the $p \times 1$ matrix denoting a truncation error on acceleration at the sample time k
$\ddot{\boldsymbol{\varepsilon}}_f(k)$	the $p \times 1$ matrix denoting a noise on acceleration due to filtering at the sample time k
$\mathbf{E}_i$	the $p \times p$ matrix denoting output energy correlation of the ith mode
F	sampling rate (Hz)
F_f	folding frequency (Nyquist frequency)
n	number of dominant poles within F_f
N	number of samples in measured time history
MAC	modal assurance criteria
mdof	multi-degrees-of-freedom
p	number of sensors
sdof	single-degrees-of-freedom
SVD	singular value decomposition
T	sampling period (s)
TDD	time domain decomposition
$\mathbf{U}$	the $p \times p$ matrix containing singular vectors of $\mathbf{Y}_i$
$\mathbf{y}(t)$	the $p \times 1$ matrix containing $y_j(t)$ with $j = 1, \ldots, p$
$y_j(t)$	displacement on the jth sensor node at time t
$\ddot{\mathbf{y}}(t)$	the $p \times 1$ matrix denoting output acceleration profile at time t
$\mathbf{Y}_i$	the $p \times N$ matrix containing mode-isolated output acceleration time histories
σ_i	noise singular values of $\mathbf{Y}_i$
$\boldsymbol{\Omega}$	the $p \times p$ diagonal matrix containing singular values of $\mathbf{Y}_i$
$\boldsymbol{\varphi}_i$	the $p \times 1$ matrix denoting the ith undamped mode shape (eigenvector)
φ_{ji}	the jth component of $\boldsymbol{\varphi}_i$
$\boldsymbol{\psi}_j$	the $p \times 1$ matrix denoting the jth noise basis
ψ_{ij}	the jth component of $\boldsymbol{\psi}_j$

such structures. In order to ensure their healthy operational condition, periodic inspection and maintenance of these structures are essential.

Remote controlled, automatic health monitoring of such systems has been recently become a popular research issue [1]. However, a prerequisite of such applications is modal testing and analysis. Ambient modal analysis techniques are particularly attractive to civil engineers, since the so-called output-only modal testing methods require no additional equipment to excite the structure being tested. Techniques that utilize ambient excitations make use of pre-existing external forces resulting from wind loading, traffic loading, and ocean waves. Consequently, output-only methods are relatively nonintrusive and inexpensive as compared to the forced excitation methods.

The peak-peaking technique [2] is one of the more widely used ambient modal analysis methods applied to the extraction of modal parameters of large civil engineering structures. Although the peak-peaking technique is straight forward, its accuracy of modal parameters

estimation is known to rely heavily on the frequency resolution. In order to overcome this drawback, many notable works have been done on the subject of the time domain. One of the memorable efforts is the Ibrahim time domain (ITD) method developed by Ibrahim [3]. The ITD method can extract modal data sets from free decay responses obtained using the random decrement (RD) technique [4]. The ITD method has been widely applied to aerospace structures by Ibrahim [5], and has been recently applied to certain civil engineering infra structures by Asmussen [6]. However, the ITD method for modal parameter extraction relies on the extracted free decay function of the response. Hence, a high level of operator interaction is required to obtain the RD function. In addition, one of difficulties of the ITD method is the occurrence of fictitious modes that are caused by either noise or other irregularities in the measured data [7]. A more advanced technique designed to overcome such difficulties is often cited in technical literature; this is Juang's [8] eigensystem realization algorithm with data correlation (ERADC) method. The ERADC method is based on the realization algorithm, which is an identification process of a discrete state-space model from a pulse-response of a system. Although the ERADC method is systematic and relatively accurate, the method still shares the difficulties of the ITD method. In addition, when a large number of time samples are collected at a large number of locations, the ERADC method requires heavy computations due to the singular value decomposition (SVD) process.

An outstanding progression in the frequency domain approach is the frequency domain decomposition (FDD) method by Brinker et al. [9]. The FDD method identifies the mode shapes and damped natural frequencies of a dynamic system by applying the SVD technique to the output spectral density matrix. This is done under an assumption of white noise excitation. The damping ratio and un-damped natural frequency are estimated from a mode-isolated, free-decay response obtained via an inverse Fourier transform of the output spectrums after applying a zero padding technique. Although the FDD method is much more advanced as compared to the peak picking method, the FDD method still requires a massive numerical computation attributable to the SVD process in the frequency domain.

Some vibration-based nondestructive damage evaluation techniques such as the damage index method by Stubbs and Kim [10] or mode shape curvature method by Pandey et al. [11] require the sufficient spatial resolution on mode shapes. Furthermore, an accurate estimation of mode shape for higher modes also requires a higher resolution of sensor spacing due to the sampling theorem. In such applications, the previously mentioned ambient modal analysis techniques may be computationally inadequate. This is because the size of the resulting system equations to be solved is associated not only with time or frequency samples, but also with the number of sensor locations. As a consequence, the large amount of numerical computation retards the real-time implementation of the previously mentioned modal analysis method. In order to overcome such shortcomings, there exists a need to develop a computationally efficient ambient modal parameter extraction technique for use in situations where a large number of sensor locations are involved. Furthermore, there is also a need to reduce the high level of operator interaction in favor of the automatic algorithm that is essential to the on-line application.

The objective of this work is to present a new technique to extract modal parameters using output-only responses when a large number of sensors are used. The following three steps are performed to achieve this objective. First, the theoretical background of the technique is presented. Second, use of the technique is demonstrated through a numerical simulation. Third,

the feasibility and practicality of the proposed technique are examined using data taken on a bridge in service.

2. Theory

2.1. Extraction of mode shapes

Linear algebra theory explains that any vector can be spanned by its basis [12]. One basis for the output response of a linear structural dynamic system consists of the underlying orthogonal mode shapes. Consider the simple beam as shown in Fig. 1. The $p \times 1$ output displacement profile vector, $\mathbf{y}(t)$, caused by an arbitrary load at time t can be spanned by mode shapes as follows

$$\mathbf{y}(t) = \sum_{i=1}^{\infty} c_i(t)\boldsymbol{\varphi}_i, \tag{1}$$

where $\mathbf{y}(t) = [y_1(t) \cdots y_p(t)]^{\mathrm{T}}$ is the displacement profile vector, and $\boldsymbol{\varphi}_i = [\varphi_{1i} \cdots \varphi_{pi}]^{\mathrm{T}}$ is the ith mode shape, and the scalar values, $c_i(t)$, denote the ith modal contribution factor of the displacement at time t. The subscript, p, denotes the number of sensors. Note that since the number of modes resolved in a continuous response of a structure is infinite, the output acceleration time history is given by

$$\ddot{\mathbf{y}}(t) = \sum_{i=1}^{\infty} \ddot{c}_i(t)\boldsymbol{\varphi}_i, \tag{2}$$

where the dot denotes differentiation with respect to time.

Suppose that the continuous acceleration response is sampled at the rate of $F(= 1/T)$ samples per second, where T denotes the sampling period. In order to prevent spectral aliasing at this stage of the sampling process, the continuous acceleration responses are assumed to be pre-filtered using low-pass analog filters limited to B Hz, where B denotes the desired bandwidth of the samples. The sampling frequency, F, is selected such that $F > 2B$. Since the sampled acceleration responses are collected at multiple sensor locations, the sequences can be classified as a multi-output system with multi-degrees-of-freedom (mdof). Under the assumption that n dominant and well-separated poles are resolved in the discrete acceleration response within the folding frequency ($F_f = F/2$), Eq. (2) can be written as

$$\ddot{\mathbf{y}}(k) = \sum_{i=1}^{n} \ddot{c}_i(k)\boldsymbol{\varphi}_i + \ddot{\boldsymbol{\varepsilon}}_t(k), \tag{3}$$

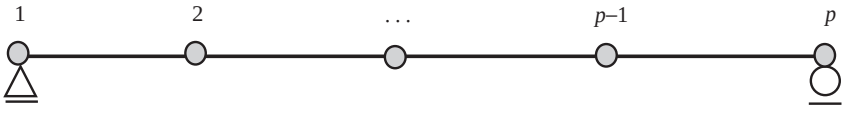

Fig. 1. Location of sensors on a beam.

where the $p \times 1$ vector, $\ddot{\boldsymbol{\varepsilon}}_t(k) = \sum_{i=n+1}^{\infty} \ddot{c}_i(k)\boldsymbol{\varphi}_i$, denotes a truncation error at the sampling time, k.

Single-degree of freedom (sdof) approaches assume that in the vicinity of a resonance, the behavior of the system is dominated by a single mode [7]. Unlike mdof approaches, sdof approaches have only a single mode and therefore have no chance of false identification of fictitious modes. This assumption reduces the level of operator interaction during on-line monitoring of modal parameters. However, most time responses measured from a real structure are a class of the mdof signal. Hence, to avoid such problems there exists a need to, as a prerequisite, extract the mode-isolated sdof signals from a mdof signal.

In the mode isolation process shown in a recent application by Farrar and James [13], the auto-spectrum magnitude on either side of a particular peak is replaced by zero. This approach requires a Fourier transformation of the time responses, and if the start and end-time samples of the measured mdof time response do not match, then leakage may occur. Hence, a high level of operator interaction is necessary and the aforementioned isolation technique may not be adequate for on-line health monitoring systems.

An alternative approach that allows circumvention of this problem is to use filter theory. A digital band-pass filter is attractive because no hardware is required [14]. Once a digital band-pass filter is properly designed for a certain frequency band that contains only a single mode, the filter can directly create sdof time responses from the measured mdof response using state-space simulation [12]. Thus, for each visually identified frequency bandwidth, a digital band-pass filter can be readily designed, and a mode-isolated discrete-time response can be created. Note that the contribution of the truncation error of the created mode isolated signal shown in Eq. (3) is insignificant. This is because the band-pass filter weighs its pass band to unity and weighs the other frequency components to zero.

If the mode-isolated signals are available, the ith filtered sdof acceleration response, $\ddot{\mathbf{y}}_i(k)$ can be given by

$$\ddot{\mathbf{y}}_i(k) = \ddot{c}_i(k)\boldsymbol{\varphi}_i + \ddot{\boldsymbol{\varepsilon}}_f(k), \tag{4}$$

where the $p \times 1$ vector, $\ddot{\boldsymbol{\varepsilon}}_f(k)$, denotes the noise at the time sample, k, due to both the band pass filtering and the residuals of $\ddot{\boldsymbol{\varepsilon}}_t(k)$. Suppose that the $p \times 1$ mode-isolated sdof acceleration vector at the sample, k, contains the modal space and orthogonal noise space. In this case, the dimension of modal space is only one (the ith mode shape vector) and the dimension of noise space is $p-1$.

The $p \times 1$ noise vector, $\ddot{\boldsymbol{\varepsilon}}_f(k)$, can be spanned by its bases at the sample time k:

$$\ddot{\boldsymbol{\varepsilon}}_f(k) = \sum_{j=1}^{p-1} \ddot{d}_j(k)\boldsymbol{\psi}_j, \tag{5}$$

where the $p \times 1$ vector,$\boldsymbol{\psi}_j = [\psi_{1j} \cdots \psi_{pj}]^{\mathrm{T}}$, denotes the jth orthogonal noise bases and scalar $\ddot{d}_j(k)$ denotes the contribution of the jth noise mode to the total noise vector at the sample time k.

By substituting Eq. (5) into Eq. (4), the mode-isolated acceleration vector at time sample k can be described as

$$\ddot{\mathbf{y}}_i(k) = \ddot{c}_i(k)\boldsymbol{\varphi}_i + \sum_{j=1}^{p-1} \ddot{d}_j(k)\boldsymbol{\psi}_j. \tag{6}$$

If N samples are measured, the matrix form of Eq. (6) becomes

$$\begin{bmatrix} \ddot{y}_{1i}(1) & \cdots & \ddot{y}_{1i}(N) \\ \vdots & \ddots & \vdots \\ \ddot{y}_{pi}(1) & \cdots & \ddot{y}_{pi}(N) \end{bmatrix} = \begin{bmatrix} \varphi_{1i} \\ \vdots \\ \varphi_{pi} \end{bmatrix} [\ddot{c}_i(1) \ \cdots \ \ddot{c}_i(N)] + \sum_{j=1}^{p-1} \begin{bmatrix} \psi_{1j} \\ \vdots \\ \psi_{pj} \end{bmatrix} \left[\ddot{d}_j(1) \ \cdots \ \ddot{d}_j(N) \right]. \tag{7}$$

Eq. (7) can be written more conveniently as

$$\mathbf{Y}_i = \boldsymbol{\varphi}_i \ddot{\mathbf{c}}_i^{\mathrm{T}} + \sum_{j=1}^{p-1} \boldsymbol{\psi}_j \ddot{\mathbf{d}}_j^{\mathrm{T}}, \tag{8}$$

where the $p \times N$ matrix, $\mathbf{Y}_i$, denotes the mode-isolated output acceleration time history that contains only the ith mode. The $N \times 1$ vector, $\ddot{\mathbf{c}}_i \equiv [\ddot{c}_i(1) \cdots \ddot{c}_i(N)]^{\mathrm{T}}$, denotes the ith modal contribution of the acceleration time response. The $N \times 1$ vector, $\ddot{\mathbf{d}}_j = [\ddot{d}_j(1) \ \cdots \ \ddot{d}_j(N)]^{\mathrm{T}}$, denotes the jth noise contribution.

Consider a cross-correlation $\mathbf{E}_i$ of the ith mode-isolated acceleration time history signals. In said case, the $p \times p$ matrix, $\mathbf{E}_i$, can be interpreted as the energy correlation of the ith mode with respect to the location of the sensors

$$\mathbf{E}_i \equiv \mathbf{Y}_i \mathbf{Y}_i^{\mathrm{T}}. \tag{9}$$

Substituting Eq. (8) into Eq. (9) yields the results

$$\mathbf{E}_i = \boldsymbol{\varphi}_i \ddot{\mathbf{c}}_i^{\mathrm{T}} \ddot{\mathbf{c}}_i \boldsymbol{\varphi}_i^{\mathrm{T}} + \boldsymbol{\varphi}_i \ddot{\mathbf{c}}_i^{\mathrm{T}} \sum_{j=1}^{p-1} \ddot{\mathbf{d}}_j \boldsymbol{\psi}_j^{\mathrm{T}} + \sum_{j=1}^{p-1} \boldsymbol{\psi}_j \ddot{\mathbf{d}}_j^{\mathrm{T}} \ddot{\mathbf{c}}_i \boldsymbol{\varphi}_i^{\mathrm{T}} + \sum_{j=1}^{p-1} \sum_{k=1}^{p-1} \boldsymbol{\psi}_j \ddot{\mathbf{d}}_j^{\mathrm{T}} \ddot{\mathbf{d}}_k \boldsymbol{\psi}_k^{\mathrm{T}}. \tag{10}$$

Now suppose that any $1 \times N$ row vector of $\mathbf{Y}_i$ in Eq. (8) consists of the modal space and the orthogonal noise space. The modal space will consist of one basis vector which denotes the ith modal contribution time history $\ddot{\mathbf{c}}_i$. The noise space will consist of $p-1$ bases which denotes the jth noise contribution factor $\ddot{\mathbf{d}}_j$ for $j = 1$ to $p-1$. For the orthogonal bases, it can be shown that [15]

$$\ddot{\mathbf{c}}_m^{\mathrm{T}} \ddot{\mathbf{c}}_n = \begin{cases} q_m, & m = n, \\ 0, & m \neq n, \end{cases} \quad \ddot{\mathbf{d}}_m^{\mathrm{T}} \ddot{\mathbf{d}}_n = \begin{cases} \sigma_m, & m = n \\ 0, & m \neq n \end{cases} \quad \text{and} \quad \ddot{\mathbf{c}}_m^{\mathrm{T}} \ddot{\mathbf{d}}_n = \ddot{\mathbf{d}}_m^{\mathrm{T}} \ddot{\mathbf{c}}_n = 0. \tag{11}$$

Therefore, Eq. (10) becomes

$$\mathbf{E}_i = \boldsymbol{\varphi}_i q_i \boldsymbol{\varphi}_i^{\mathrm{T}} + \sum_{j=1}^{p-1} \boldsymbol{\psi}_j \sigma_j \boldsymbol{\psi}_j^{\mathrm{T}}, \tag{12}$$

where the scalar values, $q_i \equiv \ddot{\mathbf{c}}_i^{\mathrm{T}} \ddot{\mathbf{c}}_i$ and $\sigma_j \equiv \ddot{\mathbf{d}}_j^{\mathrm{T}} \ddot{\mathbf{d}}_j$, physically denote the level of energy at the modes, i and j, respectively.

Eq. (12) may be rewritten as

$$\mathbf{E}_i = \mathbf{U} \boldsymbol{\Omega} \mathbf{U}^{\mathrm{T}}, \tag{13}$$

where the $p \times p$ matrix, $\mathbf{U} \equiv \lfloor \boldsymbol{\varphi}_i \quad \boldsymbol{\psi}_1 \quad \cdots \quad \boldsymbol{\psi}_{p-1} \rfloor$, is a singular vector matrix of $\mathbf{Y}_i$, and the $p \times p$ diagonal matrix, $\boldsymbol{\Omega} \equiv \mathrm{diag}\lfloor q_i \quad \sigma_1 \quad \cdots \quad \sigma_{p-1} \rfloor$, is a singular value matrix of $\mathbf{Y}_i$. The underlying assumption in the order of the singular values is that $q_i > \sigma_1 > \cdots > \sigma_{p-1}$. Therefore, the desired ith un-damped mode shape, $\boldsymbol{\varphi}_i$, which is a $p \times 1$ real vector, can be obtained by taking the first singular vector after a SVD, of $\mathbf{E}_i$ [15].

The output energy correlation matrix of the ith mode, $\mathbf{E}_i$, can be readily computed from the mode-isolated acceleration sequence by using a simple matrix multiplication in Eq. (9). The noise singular values, $\sigma_1, \ldots, \sigma_{p-1}$, should be zeros in the case of noise-free signals. For noisy signals, the noise singular values are nonzero but are small compared to q_i. The extracted singular values can be physically interpreted as an energy level of the time samples that is contributed by the corresponding mode.

For velocity and displacement response measurements, Eq. (4) can be replaced by $\dot{\mathbf{y}}_i(k) = \dot{c}_i(k)\boldsymbol{\varphi}_i + \dot{\boldsymbol{\varepsilon}}_f(k)$, and $\mathbf{y}_i(k) = c_i(k)\boldsymbol{\varphi}_i + \boldsymbol{\varepsilon}_f(k)$, respectively. Although the modal contribution factors of those measurements are of different quantities, the mode shape is the same as with the acceleration measurement. Hence, the identical procedure can be applied to the case of velocity and displacement response measurements without any loss of generality.

The described technique to extract mode shapes is subsequently refereed to as time domain decomposition (TDD). In summary, the presented TDD technique involves three steps. First, a digital band-pass filter that will isolate each target mode is designed, and the filtered time histories, $\mathbf{Y}_i$, which contain the isolated mode are generated. Second, the output energy correlation matrix, $\mathbf{E}_i$, in Eq. (9), is constructed. The SVD of the matrix $\mathbf{E}_i$, using Eq. (13), is performed next. Finally, the first column vector of the singular vector matrix, $\mathbf{U}$, is designated as the un-damped mode shape for the isolated mode.

2.2. Extraction of natural frequencies and damping ratios

Pre-multiplication of the transpose of the identified ith mode shape on Eq. (8) yields

$$\boldsymbol{\varphi}_i^{\mathrm{T}}\mathbf{Y}_i = \boldsymbol{\varphi}_i^{\mathrm{T}}\boldsymbol{\varphi}_i\ddot{\mathbf{c}}_i^{\mathrm{T}} + \boldsymbol{\varphi}_i^{\mathrm{T}}\sum_{j=1}^{p-1}\boldsymbol{\psi}_j\ddot{\mathbf{d}}_j^{\mathrm{T}}. \tag{14}$$

The second term on the right-hand side of Eq. (14) vanishes because the noise bases are assumed to be orthogonal to the modal bases. The $1 \times N$ time history vector which denotes the ith modal contribution factor of acceleration, $\ddot{\mathbf{c}}_i^{\mathrm{T}}$, can now be obtained by using Eq. (14)

$$\ddot{\mathbf{c}}_i^{\mathrm{T}} = \frac{1}{\boldsymbol{\varphi}_i^{\mathrm{T}}\boldsymbol{\varphi}_i}\boldsymbol{\varphi}_i^{\mathrm{T}}\mathbf{Y}_i. \tag{15}$$

This signal contains a single-output sdof system that represents the ith modal behavior of the acceleration for the entire set of p signals. Therefore, the auto-spectrum of $\ddot{\mathbf{c}}_i^{\mathrm{T}}$ contains one peak. The frequency at the peak is the desired damped natural frequency of the ith mode. For each mode, the traditional modal analysis methods such as the peak-peaking method or the ERADC method can be used to extract the damping ratio and natural frequency from the sdof signal, $\ddot{\mathbf{c}}_i^{\mathrm{T}}$.

Note that the orthogonal spatial noise resolved in $\mathbf{Y}_i$ is filtered out from $\ddot{\mathbf{c}}_i^{\mathrm{T}}$, which is completed by multiplying the identified mode shape vector. Also, note that the right-hand side of Eq. (15) is identical for both the displacement and velocity signal measurements. Hence, Eq. (4) is still valid for such measurements without any loss of generality.

2.3. Features of TDD

The TDD technique presented here first efficiently extracts mode shapes, and then identifies the corresponding natural frequencies. The underlying assumption of the proposed TDD technique is that the solution is separable into functions of time only and space only. Simplicity and efficiency are the fundamental advantages yielded by the separation of variables. The first step in the proposed TDD technique is only related to identification of spatial variables such as mode shape. The second step is only related to identification of temporal variables such as natural frequencies and damping ratios. Therefore, the separation of these two individual steps in the TDD technique is necessary as to share the advantages of variable separation.

Although the TDD technique requires frequency information for the filter design and natural frequency extraction, the computationally intensive part of the method deals with time domain data. In addition, the computationally intensive SVD process requires only n iterations for the $p \times p$ matrix if p signals are measured and n modes are resolved in the signals. Because the size of the SVD is dependent on the number of sensors, we can significantly save computing time and reduce required memory by using the TDD technique when $n \ll p$.

In the ERADC method, spatial variables and time variables are identified simultaneously. Consequently, the size of the block correlation Hankel matrix required for the SVD process relies on the number of sensors, length of data, and the number of correlation time lags. Hence, numerical complexity greatly increases with increases to the number of sensor locations and length of data.

Furthermore, for ideal cases, accuracy does not depend on the number of sample points or the frequency resolution to extract mode shapes. Thus, the identified mode shapes converge very quickly with respect to the number of sample points. Therefore, the TDD technique is especially useful for ambient modal analysis of large structures because their lower frequencies are of interest in the most engineering applications. Also, the TDD technique may be implemented in real-time applications since the filtering preprocess for mode isolation can be realized by means of an electronic circuit and a simple SVD.

3. Numerical example

Consider the simple supported beam shown in Fig. 1. The length of the beam is 30 m, and 11 accelerometers ($p = 11$) are placed on the beam with an equal spacing of 3 m. The second moment of cross-sectional area, Young's modulus, and density of the beam are $1.0\,\mathrm{m}^4$, 20 GPa, and $2.7 \times 10^3\,\mathrm{kg/m}^3$, respectively. The finite element (FE) model consists of 100 linear elements (101 nodes), each with a uniform length of 0.3 m. From the FE analysis, the un-damped natural

frequencies for the first, second, and third bending modes are 1.98, 7.90, and 17.78 Hz, respectively.

Given a unit pulse load at the third sensor, the acceleration time responses at all of the sensors are simulated using the FE software package ABAQUS® [16]. The simulation makes use of the modal superposition technique after the completion of an eigenvalue analysis of the structure. The damping ratio used here is 0.015 (a typical value for lightly damped structures) for all modes. With a sampling period of $T = 0.015$ sec, the 1024 samples ($N = 1024$) of transverse degrees of freedom are collected at the 11 sensor locations. The typical acceleration time history and its corresponding auto spectrum at the fourth node are shown in Figs. 2 and 3, respectively.

The first step of the process involves designing a digital band-pass filter for each of the three modes. As shown in Fig. 3, the first three peaks range from 1 to 3 Hz, from 7 to 9 Hz, and from 17

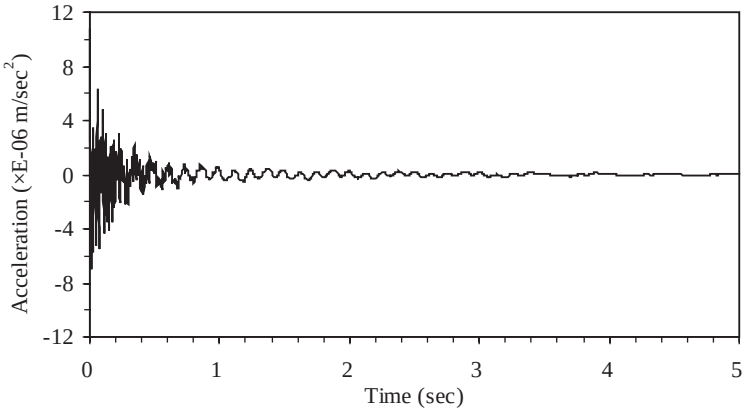

Fig. 2. Acceleration at the fourth node of the beam.

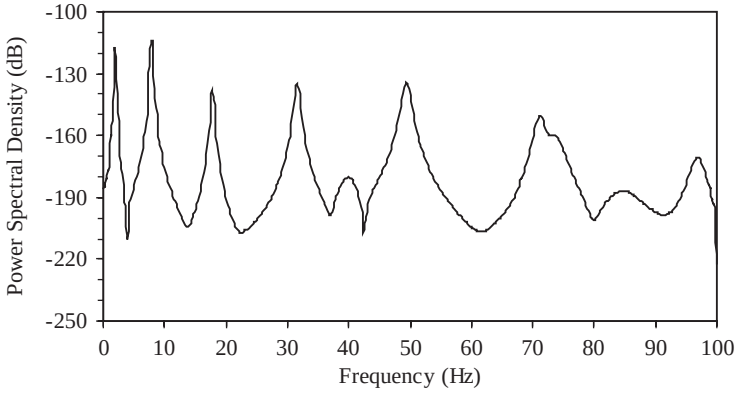

Fig. 3. Power spectral density of acceleration at the fourth node of the beam.

to 19 Hz, respectively. A third-order Butterworth digital band-pass filter is designed for each frequency range. Three 11×1024 sets of mode-isolated time histories are created using a linear system theory such as a discrete state space simulation [12].

Next, for each mode-isolated time history, the matrix multiplication in Eq. (9) is performed. The three resulting 11×11 matrices denote the energy correlation of each mode with respect to the sensors spatial coordinates.

The next step involves performing a SVD analysis on each of the energy correlation matrices in Eq. (13). Note that the size of matrix for the SVD analysis is only 11×11 for each mode. For each mode, the 11×1 un-damped mode shapes vector is extracted by taking the first column vector from the quantity $\mathbf{U}$ in Eq. (13).

The first three bending mode shapes to be identified are shown in Fig. 4. For the first three bending modes, the modal assurance criteria (MAC) values between the estimated mode shape and the eigenvector from the FE analysis are 1.000, 1.000, and 0.999, respectively. For each mode, the extracted singular values imply the level of noise in the signal. Thus the quantification of noise in the signal is a feasible task by means of inspecting the singular values. For the extracted three bending modes, the ratios of the second singular values to first singular values are 0.27%, 0.46%, and 6.30%, respectively. Theoretically the ratios should be equal to zeros, so one may say that the numerical noises are involved with such levels in the time response simulation.

The final step in the extraction of the natural frequency for each mode is to compute a single representative sdof time history in Eq. (15). The ERADC method identifies the first three natural frequencies are 1.98, 7.90, and 17.78 Hz, respectively. The corresponding damping ratios from the ERADC method are exactly 1.5% for all the three modes. Using the peak peaking method, the first three damped natural frequencies with a frequency resolution of 0.1953 Hz are 1.95, 7.81, and 17.77 Hz, respectively. The corresponding damping ratios determined with Half-Power Bandwidth method are 2.08%, 0.25%, and 0.04%, respectively.

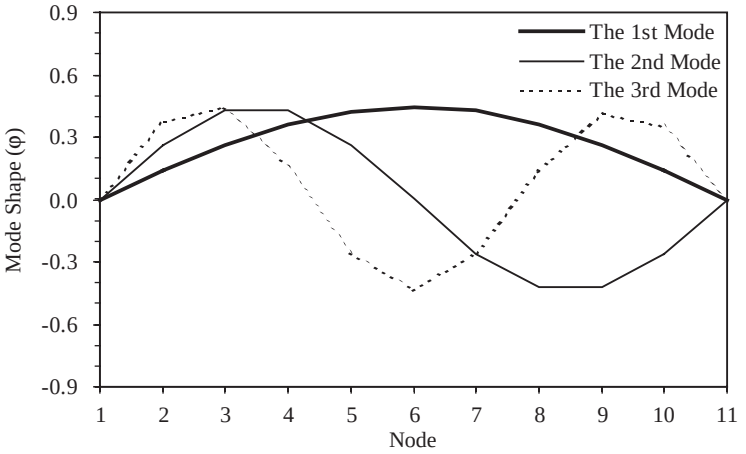

Fig. 4. The estimated first three bending mode of the beam using TDD.

4. Field verification

4.1. Description of test structure

The King Storm Water Bridge is a two-span-reinforced concrete bridge located in the high desert of Southern California in the United States. The temperature extremes exhibited at the site are 49 °C in the summer and near freezing temperature in the winter. Daily temperature variations are between 6 °C and 1 °C [17]. The bridge has a standard CALTRANS (California Department of Transportation) reinforced monolithic cast-in-place slab deck design. The deck is 0.43 m thick and 13.1 m wide, and is supported by two rigidly connected abutment walls and by six uniformly spaced 380 mm diameter pre-stressed concrete columns at mid-span. Each span of the deck is 10.0 m long. The abutment walls are 0.77 m thick × 2.0 m deep and are supported by five 380 mm diameter pre-stressed concrete piles. The CALTRANS Type 25 reinforced concrete barrier rails are placed along the longitudinal edges of the bridge, as depicted in Fig. 5.

4.2. Description of modal test

A roving sensor technique was conducted to record time data. Seven sets of a forced vibration test (A, B, C, D, E, F, and G in Fig. 5) were scheduled to record 28 acceleration time responses and force inputs. The reference point and an impact point were 'A3' and 'I1' shown in Fig. 5, respectively.

Five PCB 393A03 ICP model accelerometers and a custom-made drop hammer were used to obtain force time histories. The hammer tip was instrumented with 9.09 kN PCB 200C20

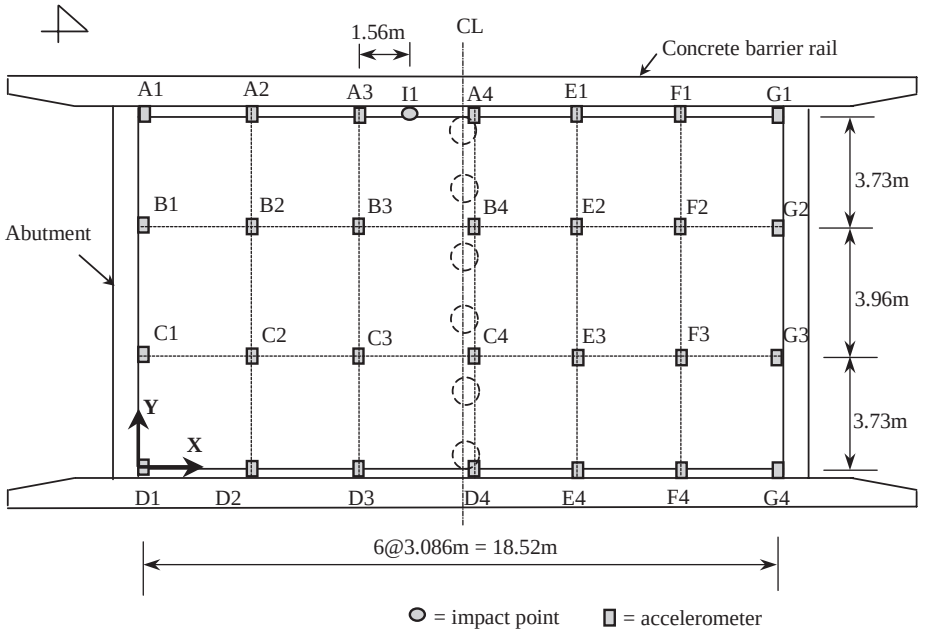

Fig. 5. Plan view and sensor layout of King Storm Water Bridge.

piezoelectric load cell. The time data were acquired and processed with an eight-channel Zonic Model 2300 signal analyzer. The sampling rate of the data logger was set to 1280 Hz. Each sensor recorded 5000 samples for each data set. A typical acceleration time history at node "B3" is shown in Fig. 6. All the power spectrum densities are shown in Fig. 7. A typical coherence function of nodes "B3" and "C3" are shown in Fig. 8. The first seven frequencies are between 5 and 40 Hz.

4.3. Output-only modal analysis using proposed method

Using only output acceleration time histories measured with the roving sensor technique to extract mode shapes, natural frequencies and damping ratios first requires scaling the acceleration

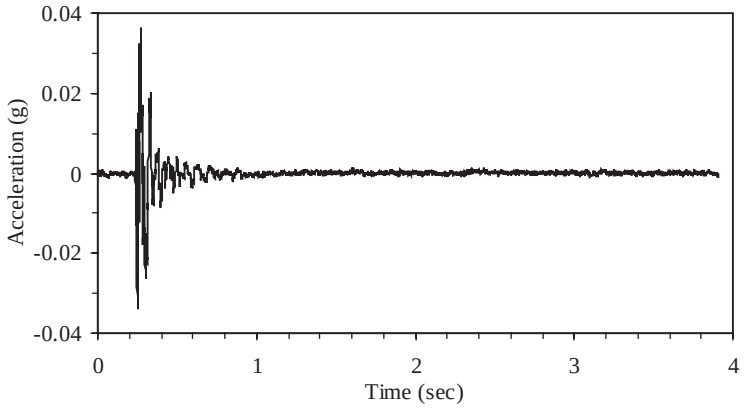

Fig. 6. Acceleration at node B3 due to impact load at node I1 of the bridge.

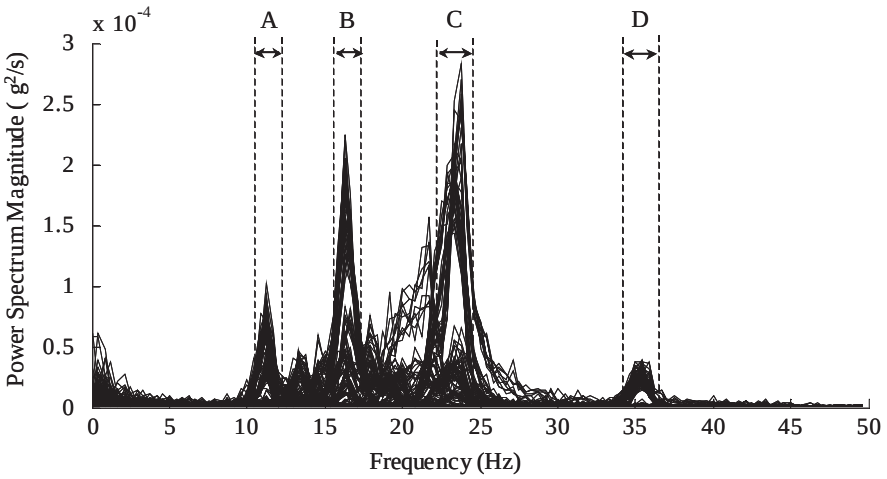

Fig. 7. Power spectrums of sampled accelerations due to impact load at node I1 of the bridge.

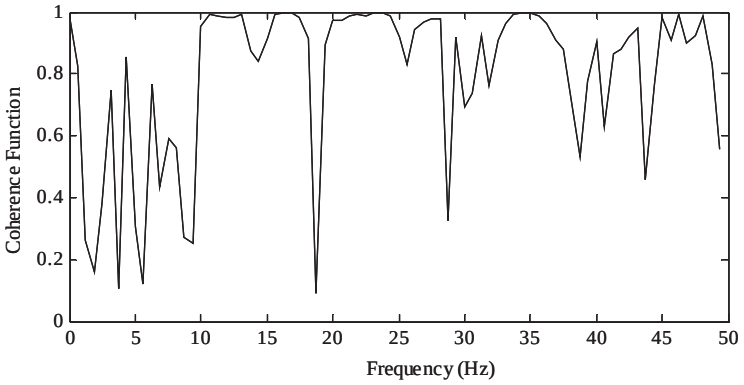

Fig. 8. Coherence function of node B3 and node C3

signals with respect to the reference time history. This is because the magnitude of input can be arbitrary for each test set. The scaling processes consist of the following three steps: (1) Compute transfer functions between a reference point and the other points. (2) For each transfer function, replace the frequency components with zero except when the frequency is between 5 and 40 Hz. (3) Compute the scaled time history by taking the inverse discrete Fourier transformation of the frequency filtered transfer function. Then the 28×5000 scaled acceleration time matrix can be constructed by putting together the 28 scaled acceleration responses. Next, the third-order Butterworth digital band-pass filters are designed for the band-pass zones of A (11–12 Hz), B (16–17 Hz), C (23–24 Hz), and D (35–36 Hz) as shown in Fig. 7. Here, the pass bands of the digital filter are determined by inspecting the spectrums and the coherence functions of accelerations shown in Figs. 7 and 8, respectively. The peaks are commonly observed at above selected bandwidths in all the measured accelerations. For each designed filter, the 28×5000 mode-isolated scaled acceleration matrix is simulated in discrete state space. The typical spectrums of mode-isolated sdof signals for the first pass band are shown in Fig. 9. After computing the 28×28 energy correlation matrix from Eq. (9) for each mode, the SVD of each energy correlation matrix exhibits an un-damped mode shape. The four estimated mode shapes are depicted in Figs. 10–13. After using Eq. (15) to project the mode-isolated time signals on each previously identified modal space, the un-damped natural frequencies are extracted using the ERADC technique, and are 11.06, 16.93, 23.02, and 35.36 Hz, respectively. The corresponding damping ratios are 1.87%, 1.26%, 2.3%, and 0.36%, respectively. In order to compare the performance of the TDD technique with a classic modal analysis method, the ME'scopeVES [18], an automated software package for modal analysis of forced vibration tests, was used to extract modal parameters from the test data. The rational fraction polynomial (RFP) method by Richardson and Formenti [19] was applied to each set of test data consisting of inputs and outputs. For the frequency zone used in the TDD, the estimated first natural frequencies using the RFP method were 11.17, 16.40, 23.31, and 35.36 Hz, respectively. For the four extracted mode shapes, the MAC values between the TDD technique and the classic modal analysis were 0.98, 0.82, 0.85, and 0.90, respectively.

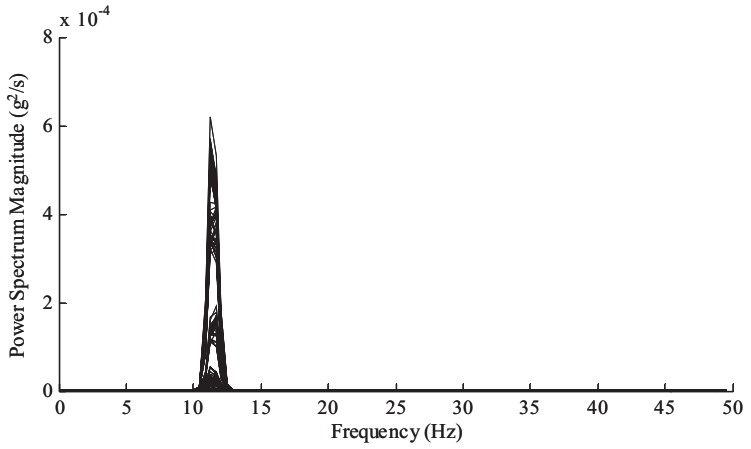

Fig. 9. Power spectrums of the mode-isolated signals through a band-pass filter (11–12 Hz).

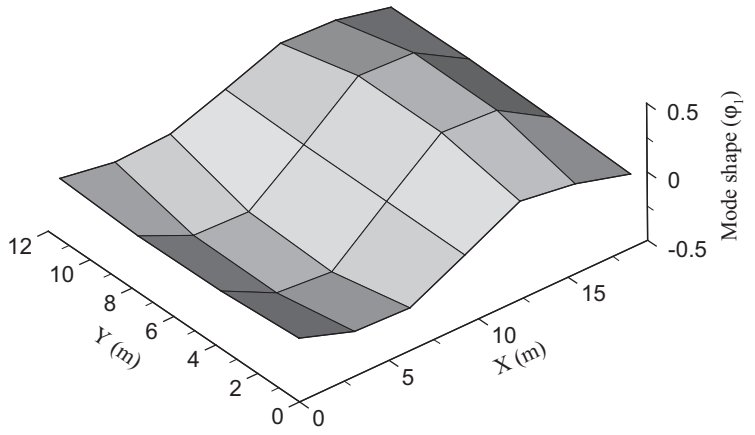

Fig. 10. The first mode shape of the bridge using the TDD technique.

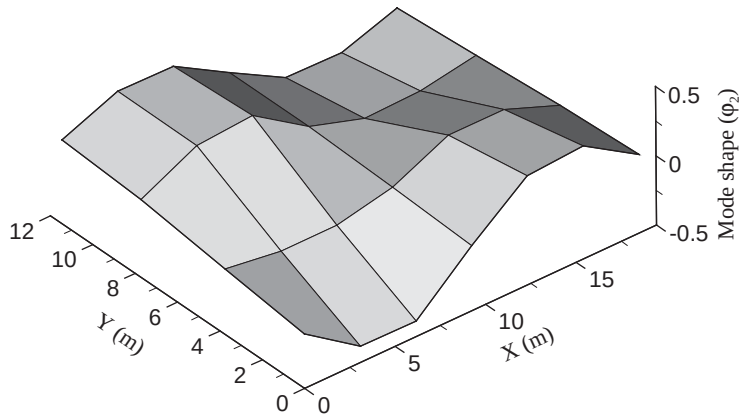

Fig. 11. The second mode shape of the bridge using the TDD technique.

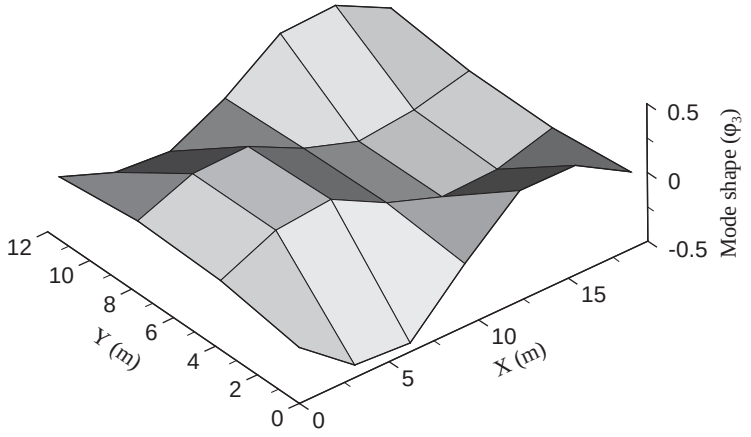

Fig. 12. The third mode shape of the bridge using the TDD technique.

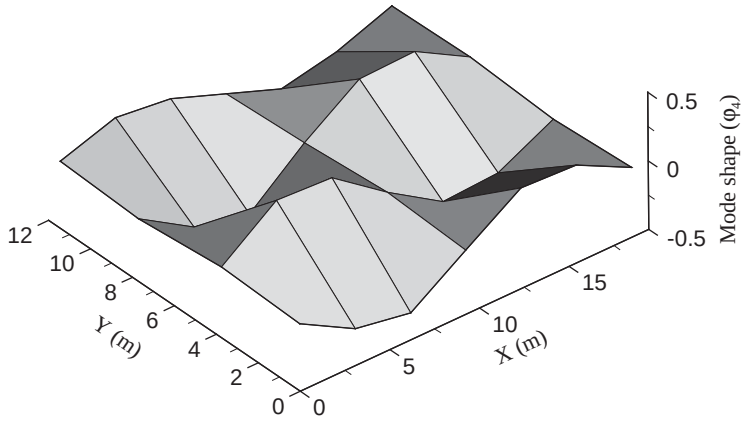

Fig. 13. The fourth mode shape of the bridge using the TDD technique.

5. Summary and conclusions

The objective of this work is to develop an ambient modal analysis method that may be efficient when a large number of sensor nodes are involved. Three tasks are conducted to achieve the objective. First, the theoretical developments of the proposed method are presented. Second, the proposed method is verified by a numerical study. Third, the feasibility and practicality are examined through ambient modal testing of a bridge in service.

Based on results and interpretations, the following three findings and conclusions can be addressed. First, the SVD matrix size of the proposed method relies on the number of sensors instead of the number of time samples or frequency samples. Therefore, the proposed approach is adequate to obtain spatially refined mode shapes. Second, the formulation of the proposed method includes no assumption for the inputs. Therefore, the proposed method can extract undamped mode shapes for the arbitrary inputs related to the extraction of mode shapes. Third, the mode isolation task completed by using a digital band-pass filter reduces the normally high level

of operator interaction. Therefore, the proposed method can be applied to an automated on-line health-monitoring system.

Despite its strong points, the TDD technique also has at least two limitations based on its theoretical foundation. First, the proposed method is based on the sdof approach. Therefore, as with other sdof methods, the extraction of modal parameters from closely placed modes is difficult. However, the modes of typical civil engineering structures are well separated. Second, the proposed method utilizes a mode-isolated time signal to extract natural frequencies. Therefore, the band-pass filters may bias the damping estimation if the width of the pass band of the filter is too thin.

References

[1] S.W. Doebling, C.R. Farrar, M.B. Prime, A summary review of vibration-based damage identification methods, *The Shock and Vibration Digest* 30 (2) (1998) 91–105.
[2] J.S. Bendat, A.G. Piersol, *Engineering Applications of Correlation and Spectral Analysis*, Wiley, New York, 1980 pp. 181–186.
[3] S.R. Ibrahim, E.C. Mikulcik, A method for the direct identification of vibration parameters from the free response, *Shock and Vibration Bulletin* 47 (4) (1977) 183–198.
[4] J.K. Vandiver, A.B. Dunwoody, R.B. Campbell, M.F. Cook, A mathematical basis for the random decrement vibration signature analysis technique, *Journal of Mechanical Design* 104 (1982) 307–313.
[5] S.R. Ibrahim, Random decrement technique for identification of structures, *Journal of Spacecraft* 14 (11) (1977) 696–700.
[6] J.C. Asmussen, Modal Analysis Based on the Random Decrement Technique-Application to Civil Engineering Structures, PhD Thesis, Aalborg University, Denmark, 1997.
[7] D.J. Ewins, *Modal Testing: Theory, Practice and Application*, ed, Research Studies Press, Hertfordshire, England, 2000.
[8] J.-N. Juang, *Applied System Identification*, Prentice-Hall, Englewood Cliffs, NJ, 1994, pp. 133–147.
[9] R. Brinker, L. Zhang, P. Andersen, Modal identification from ambient responses using frequency domain decomposition, *Proceedings of 18th International Modal Analysis Conference*, San Antonio, TX, 2000, pp. 625–630.
[10] N. Stubbs, J.T. Kim, Damage localization in structures without baseline modal parameters, *AIAA Journal* 34 (8) (1996) 1644–1649.
[11] A.K. Pandey, M. Biswas, M.M. Samman, Damage detection from changes in curvature mode shapes, *Journal of Sound and Vibration* 145 (2) (1991) 321–332.
[12] C.-T. Chen, *Linear System Theory and Design*, Third ed, Oxford University Press, New York, 1999.
[13] C.R. Farrar, G.H. James III, System identification from ambient vibration measurements on a bridge, *Journal of Sound and Vibration* 205 (1) (1997) 1–18.
[14] J.G. Proakis, D.G. Manolakis, *Digital Signal Processing: Principles, Algorithms, and Applications*, ed, Prentice-Hall, Eaglewood Cliffs, NJ, 1996.
[15] G.H. Golub, C.F. Van Loan, *Matrix Computations*, ed, The Johns Hopkins University Press, Baltimore, MD, 1996, p. 70.
[16] ABAQUS/Standard User's Manual—version 6.2, Hibbit, Karlson & Sorenson, Pawtucker, RI, 2002.
[17] R. Bolton, N. Stubbs, C. Sikorsky, Automation of modal property extraction for a permanently instrumented highway bridge, *Proceedings of the 20th International Modal Analysis Conference*, Los Angeles, CA, 2002, pp. 1217–1223.
[18] ME'scopeVES Operating Manual—version 3.0, Vibrant Technology Inc., Jamestown, CA, 2001.
[19] M.H. Richardson, D.L. Formenti, Global curve-fitting of frequency response measurements using the rational fraction polynomial method, *Proceedings of the Third International Modal Analysis Conference*, Orlando, FL, 1985, pp. 390–397.